

Supporting Information

for

A Three-Coordinate and Quadruply Bonded Mo–Mo Complex

Yi-Chou Tsai,^{a,*}, Yang-Miin Lin,^a Jen-Shiang K. Yu,^b and
Jenn-Kang Hwang^b

^aDepartment of Chemistry, National Tsing Hua University, Hsinchu 300, Taiwan,

^bDepartment of Biological Science and Technology, National Chiao Tung University,
Hsinchu 300, Taiwan

E-mail: yictsa@mx.nthu.edu.tw

Experimental

General Information. Unless stated otherwise, all operations were performed using standard Schlenk techniques or in a Vacuum Atmospheres dry box under an atmosphere of nitrogen. Diethyl ether (Et_2O) and tetrahydrofuran (THF) were distilled under nitrogen from purple sodium benzophenone ketyl. Hexane was distilled under nitrogen from CaH_2 . Distilled solvents were transferred under vacuum into vacuum-tight glass vessels before being transferred into a drybox. C_6D_6 was purchased from Aldrich and was degassed and dried over 4 Å sieves. The 4 Å sieves and Celite were dried in vacuo overnight at a temperature just above 200 °C. $\text{MoCl}_3(\text{THF})_3$ ¹ was prepared following literature method. All other compounds were used as received. ^1H and ^{13}C NMR spectra were recorded on Varian Unity INOVA 500 MHz or Bruker DMX 600 MHz spectrometers at room temperature. ^{13}C NMR spectra are proton decoupled. Chemical shifts are reported with respect to internal solvent: 7.16 ppm and 128.00(t) ppm (C_6D_6). UV-vis absorption spectra were collected on a JASCO V-570 UV/VIS/NIR spectrophotometer. Resonance Raman spectrum was recorded with a confocal Labram instrument of the Jobin Yvon–Horiba (Triax 550 spectrometer), equipped with a He–Ne laser at 632.8 nm ($E_{\text{laser}} = 2.41\text{eV}$) and a liquid nitrogen cooled CCD detector (1024×256) with 1024 pixels. The spectrum was recorded in backscattering after focalisation in several positions within a small area (ca. $5\text{ }\mu\text{m} \times 5\text{ }\mu\text{m}$) of the compound powder, and the maximum power employed was 5mW. CHN analyses were performed by Precious Instrument Center at National Chiao Tung University (Hsinchu, Taiwan) with a Heraeus CHN-O-Papid elemental analyzer.

Synthesis of $\text{Mo}_2\text{Cl}_2(\mu\text{-}\eta^2\text{-Me}_2\text{Si(NDipp)}_2)_2$ (1**).** In a vial was prepared a suspension of $\text{MoCl}_3(\text{THF})_3$ in 10 mL of diethyl ether and kept at -35°C for 30 min. To the orange suspension was slowly added solid $\text{Li}_2[\text{Me}_2\text{Si(NDipp)}_2]$ at -35°C . As the reaction mixture was allowed to warm to room temperature, a slow darkening of solution to orange brown was observed in 1 hr. Stirring was continued at room temperature overnight, at which point, it was filtered through Celite and all volatiles were removed to dryness under vacuum. Recrystallization from hexane at -35°C furnished **1** as orange crystals. Yield: (2 crops 90%). ^1H NMR (600 MHz, C_6D_6): δ 7.49 (dd, 4H, Dipp meta), 7.14 (dd, 4H, Dipp para), 7.09 (dd, 4H, Dipp meta), 4.28 (septa, 4H, CHMe_2), 4.18 (septa, 4H, CHMe_2), 1.71 (d, 12H, CMe_2), 1.48 (d, 12H, CMe_2), 1.30 (d, 12H, CMe_2), 0.63 (d, 12H, CMe_2), 0.35 (s, 12H, SiMe_2). ^{13}C NMR (126 MHz, C_6D_6): δ 143.3 (C, Dipp ortho), 142.7 (C, Dipp ortho), 129.4 (CH, Dipp meta), 128.3 (C, Dipp ipso), 128.1 (CH, Dipp meta), 125.1 (CH, Dipp para), 41.6 (CH, CHMe_2), 33.2 (CH, CHMe_2), 29.9 (CH_3 , SiMe_2), 27.3 (CH_3 , CMe_2), 27.2 (CH_3 , CMe_2), 24.7 (CH_3 , CMe_2), 23.2 (CH_3 , CMe_2). Anal. Calcd for $\text{C}_{52}\text{H}_{80}\text{N}_4\text{Cl}_2\text{Si}_2\text{Mo}_2$: C, 57.82; H, 7.47; N, 5.19; Found: C, 58.13; H, 7.80; N, 5.65.

Synthesis of $\text{Mo}_2[\mu\text{-}\eta^2\text{-SiMe}_2\text{(NDipp)}_2]_2$ (2**).** A 0.40% Na/Hg was prepared by dissolving Na metals (80 mg, 3.48 mmol) in Hg in a 20 mL scintillation vial. THF was added (10 mL) and the amalgam was stirred for 10 min, followed by addition of solid orange **1** (1.86 g, 1.72 mmol) at room temperature. Vigorous stirring was continuing overnight and the color remained orange. The solution was filtered through Celite, and solvent was removed in vacuo from the filtrate, yielding an orange solid. Recrystallization from hexane at -35°C furnished **2** as orange brown crystals (43% yield in two crops). ^1H NMR (500 MHz, C_6D_6): δ 7.28 (d, 4H, Dipp meta), 7.17 (d, 4H, Dipp meta), 7.06 (t, 2H, Dipp para), 6.98 (t, 2H, Dipp para), 4.20 (septet, 4H, CHMe_2), 3.76 (septet, 4H, CHMe_2), 1.39 (d, 24H, CMe_2), 1.28 (d, 24H, CMe_2), 0.37 (s, 12H,

SiMe₂). ¹³C NMR (126MHz, C₆D₆): δ = 142.1 (C, Dipp ortho), 141.5 (C, Dipp ipso), 123.5 (CH, Dipp meta), 122.8 (CH, Dipp meta), 116.3 (CH, Dipp para), 28.4 (CH, CHMe₂), 27.4 (CH, CHMe₂), 25.1 (CH₃, CMe₂), 24.1 (CH₃, CMe₂), 3.67 (CH₃, SiMe₂). Resonance Raman: 343 cm⁻¹. MS (FAB): m/z (relative intensity, %): [M] 1012 (2.65). Anal. Calcd for C₅₂H₈₀N₄Si₂Mo₂: C, 61.88; H, 7.99; N, 5.55. Found: C, 61.50; H, 8.12; N, 5.08.

Crystallographic Structure Determinations. The X-ray crystallographic data collections for **1** and **2** were carried out on a Bruker-Nonius Kappa CCD four-circle diffractometer with graphite-monochromated Mo Kα radiation ($\lambda = 0.71073 \text{ \AA}$) outfitted with a low-temperature, nitrogen-stream aperture. The structures were solved using direct methods, in conjunction with standard difference Fourier techniques and refined by full-matrix least-squares procedures. A summary of the crystallographic data for complexes **1** and **2** is shown in Table S1. An empirical absorption correction (multi-scan) was applied to the diffraction data for all structures. All non-hydrogen atoms were refined anisotropically. Unless otherwise specified, all hydrogen atoms were calculated by using the riding model. All software used for diffraction data processing and crystal-structure solution and refinement are contained in the SIR92 or SHELXL 97 program suites, respectively.

Computational Details. All of the molecular structures were optimized using BLYP density functional theory (DFT) with the LANL2DZ basis set employing Hay and Wadt's LANL2 effective core potentials (ECP) applied to Mo and Si atoms, resulting in respectively 1086 and 1090 Cartesian basis functions for **2** and **2(μ-H)₂**. Zero-point energy correction as well as time-dependent DFT (TDDFT)² computations were followed at the identical level of theory using corresponding optimized geometries. All of the calculations were done using Gaussian 03 program.³

References

1. Stoffelbach, F.; Saurenz, D.; Poli, R. *Euro. J. Inorg. Chem.* **2001**, 2699-2703.
2. (a) Stratmann, R. E.; Scuseria, G. E.; Frisch, M. J. *J. Chem. Phys.* **1998**, *109*, 8218–8224. (b) Casida, M. E.; Jamorski, C.; Casida, K. C.; Salahub, D. R. *J. Chem. Phys.* **1998**, *108*, 4439–4449.
3. Frisch, M. J.; Trucks, G. W.; Schlegel, H. B.; Scuseria, G. E.; Robb, M. A.; Cheeseman, J. R.; Montgomery, J. A.; Vreven, Jr., T.; Kudin, K. N.; Burant, J. C.; Millam, J. M.; Iyengar, S. S.; Tomasi, J.; Barone, V.; Mennucci, B.; Cossi, M.; Scalmani, G.; Rega, N.; Petersson, G. A.; Nakatsuji, H.; Hada, M.; Ehara, M.; Toyota, K.; Fukuda, R.; Hasegawa, J.; Ishida, M.; Nakajima, T.; Honda, Y.; Kitao, O.; Nakai, H.; Klene, M.; Li, X.; Knox, J. E.; Hratchian, H. P.; Cross, J. B.; Adamo, C.; Jaramillo, J.; Gomperts, R.; Stratmann, R. E.; Yazyev, O.; Austin, A. J.; Cammi, R.; Pomelli, C.; Ochterski, J. W.; Ayala, P. Y.; Morokuma, K.; Voth, G. A.; Salvador, P.; Dannenberg, J. J.; Zakrzewski, V. G.; Dapprich, S.; Daniels, A. D.; Strain, M. C.; Farkas, O.; Malick, D. K.; Rabuck, A. D.; Raghavachari, K.; Foresman, J. B.; Ortiz, J. V.; Cui, Q.; Baboul, A. G.; Clifford, S.; Cioslowski, J.; Stefanov, B. B.; Liu, G.; Liashenko, A.; Piskorz, P.; Komaromi, I.; Martin, R. L.; Fox, D. J.; Keith, T.; Al-Laham, M. A.; Peng, C. Y.; Nanayakkara, A.; Challacombe, M.; Gill, P. M. W.; Johnson, B.; Chen, W.; Wong, M. W.; Gonzalez, C.; Pople, J. A. *Gaussian 03, Revision C.02*; Gaussian, Inc.: Wallingford CT, 2004.

Table S1. Crystallographic Data for **1** and **2**

compound	1	2
empirical formula	C52H80Cl2N4Si2Mo2	C52H80N4Si2Mo2
fw	1080.16	1009.26
crystal system	Orthorhombic	Monoclinic
space group	Fdd2	P2 ₁ /n
a (Å)	28.2680(6)	12.2370(2)
b (Å)	35.3567(10)	18.6080(4)
c (Å)	10.8372(2)	12.8100(3)
β (deg)	90	115.0730(10)
Vol (Å ³)	10831.4(4)	2642.05(9)
Z	8	2
d (calc. g/cm3)	1.325	1.269
μ (mm ⁻¹)	0.643	0.556
temperature (K)	200	200
final R indices	R1 = 0.0400	R1 = 0.0701
[I > 2σ(I)]a,b	wR2 = 0.0899	wR2 = 0.1603
R indices	R1 = 0.0511	R1 = 0.0777
(all data)	wR2 = 0.0956	wR2 = 0.1654

^aR1 = $\sum ||F_o| - |F_c|| / \sum |F_o|$. ^bwR2 = $[\sum [w(F_o^2 - F_c^2)^2] / \sum w(F_o^2)^2]^{1/2}$, $w = 1/[\sigma^2(F_o^2) + (aP)^2 + bP]$, where $P = [\max(F_o^2 \text{ or } 0) + 2(F_c^2)]/3$

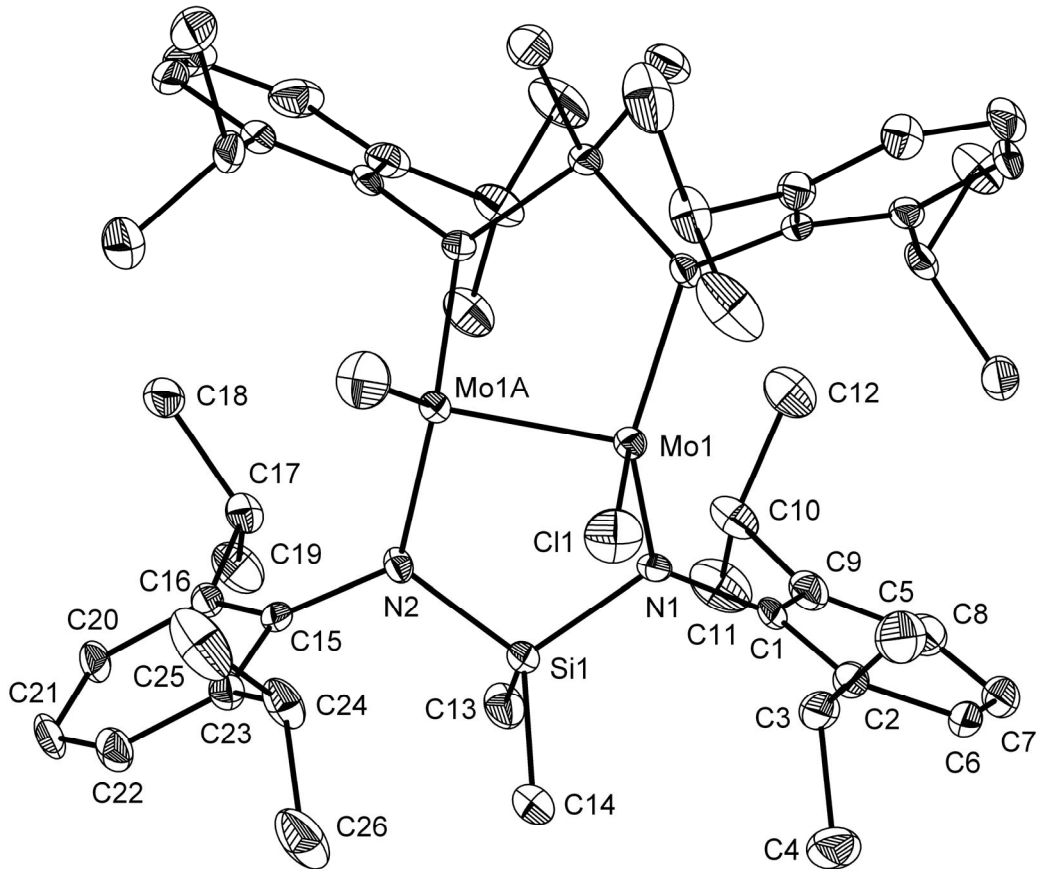


Figure S1. ORTEP diagram of complex 1 with ellipsoids at the 30% probability level. Selected bond distances (\AA) and angles (deg): Mo(1)–Mo(1A), 2.2013(8); Mo(1)–N(1), 1.988(4); Mo(1A)–N(2), 1.976(4); Mo(1)–Cl(1), 2.3136(15); Si(1)–N(1), 1.770(4); Si(1)–N(2), 1.761(4); N(1)–Mo(1)–N(2A), 127.03(15); N(1)–Mo(1)–Mo(1A), 96.67(12); N(2)–Mo(1A)–Mo(1), 96.90(11); N(1)–Mo(1)–Cl(1), 110.65(12); N(2)–Mo(1A)–Cl(1A), 116.91(11); Cl(1)–Mo(1)–Mo(1A), 99.90(5); N(1)–Si(1)–N(2), 104.47(19); C(1)–N(1)–Mo(1), 125.8(3); Si(1)–N(1)–Mo(1), 117.2(3).

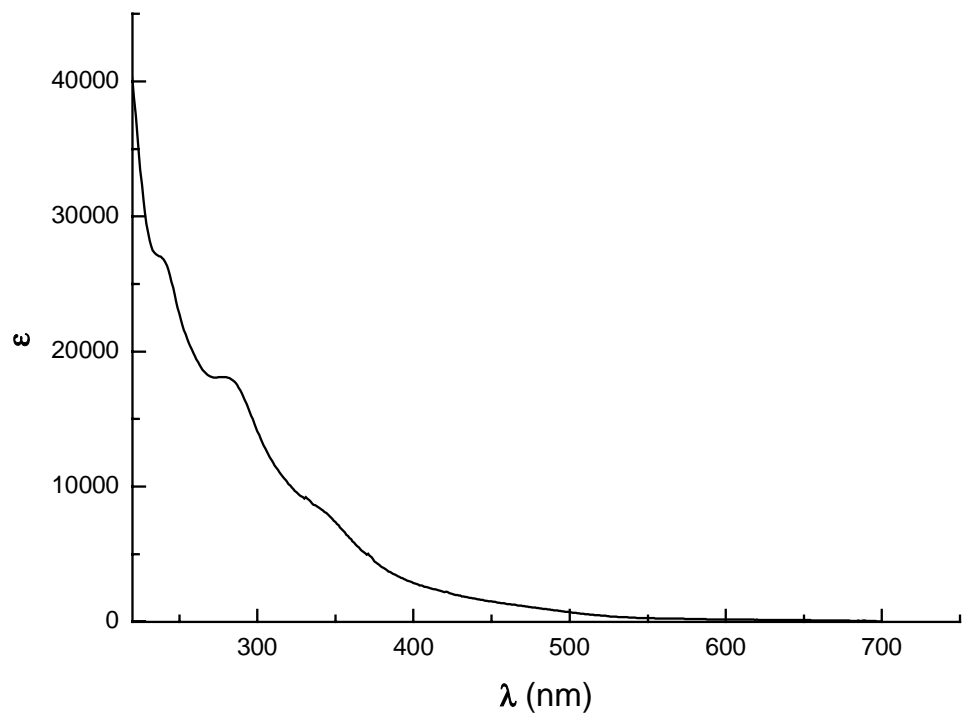


Figure S2. UV-vis spectrum of **1**.

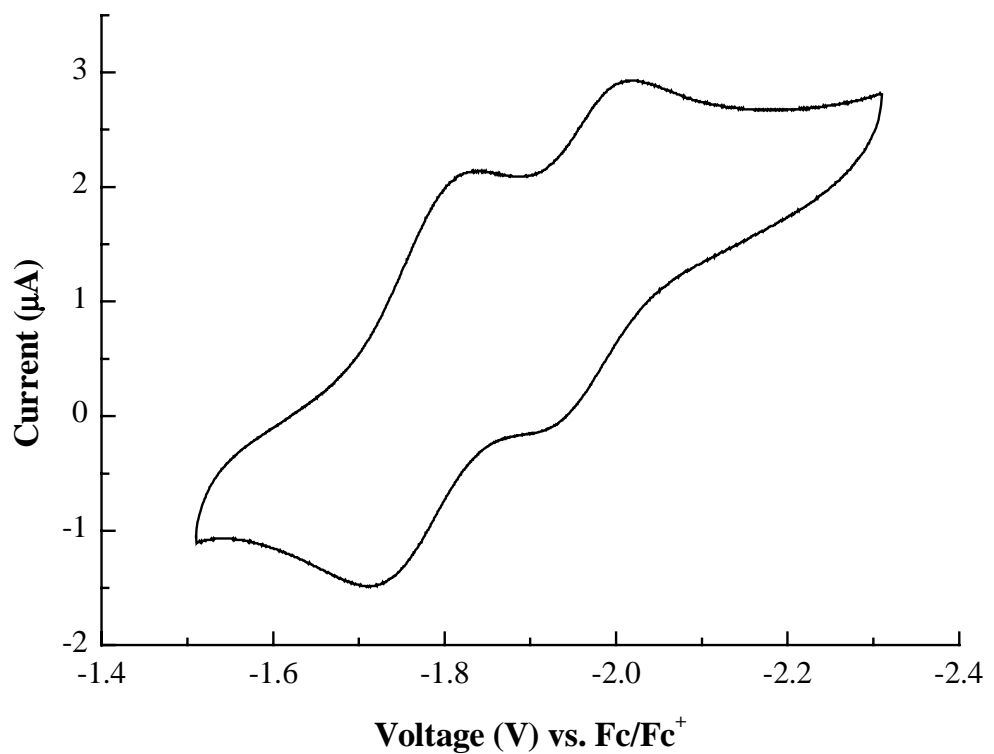


Figure S3. Cyclic voltammogram of **1** recorded un THF solution containing 0.50 M TBAP. Scan rate is 0.10 V s⁻¹.

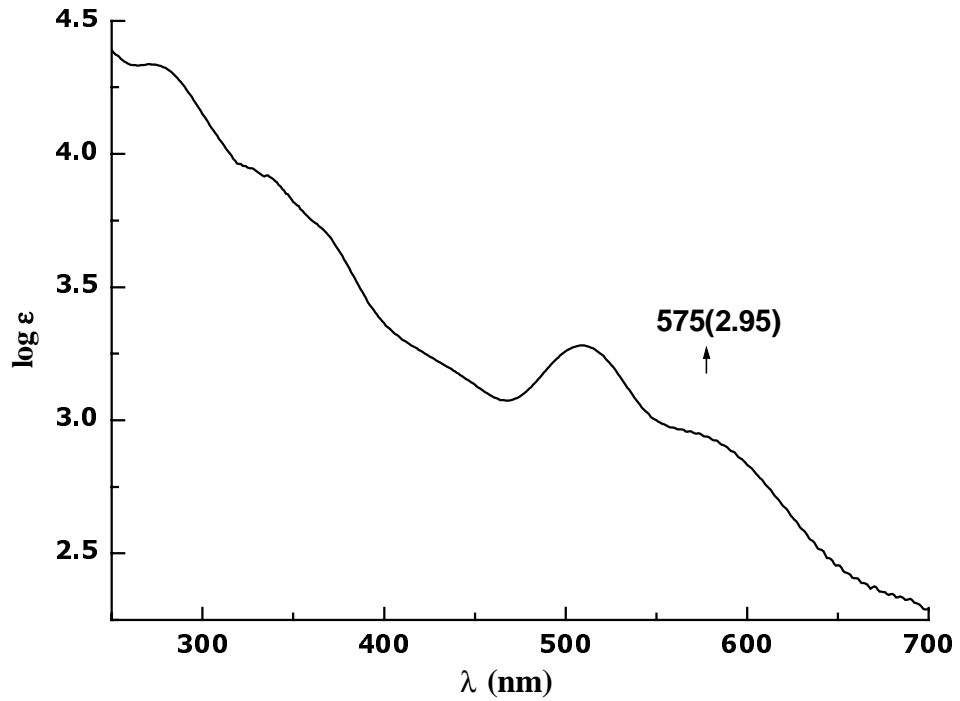


Figure S3. UV-vis spectrum of 2.

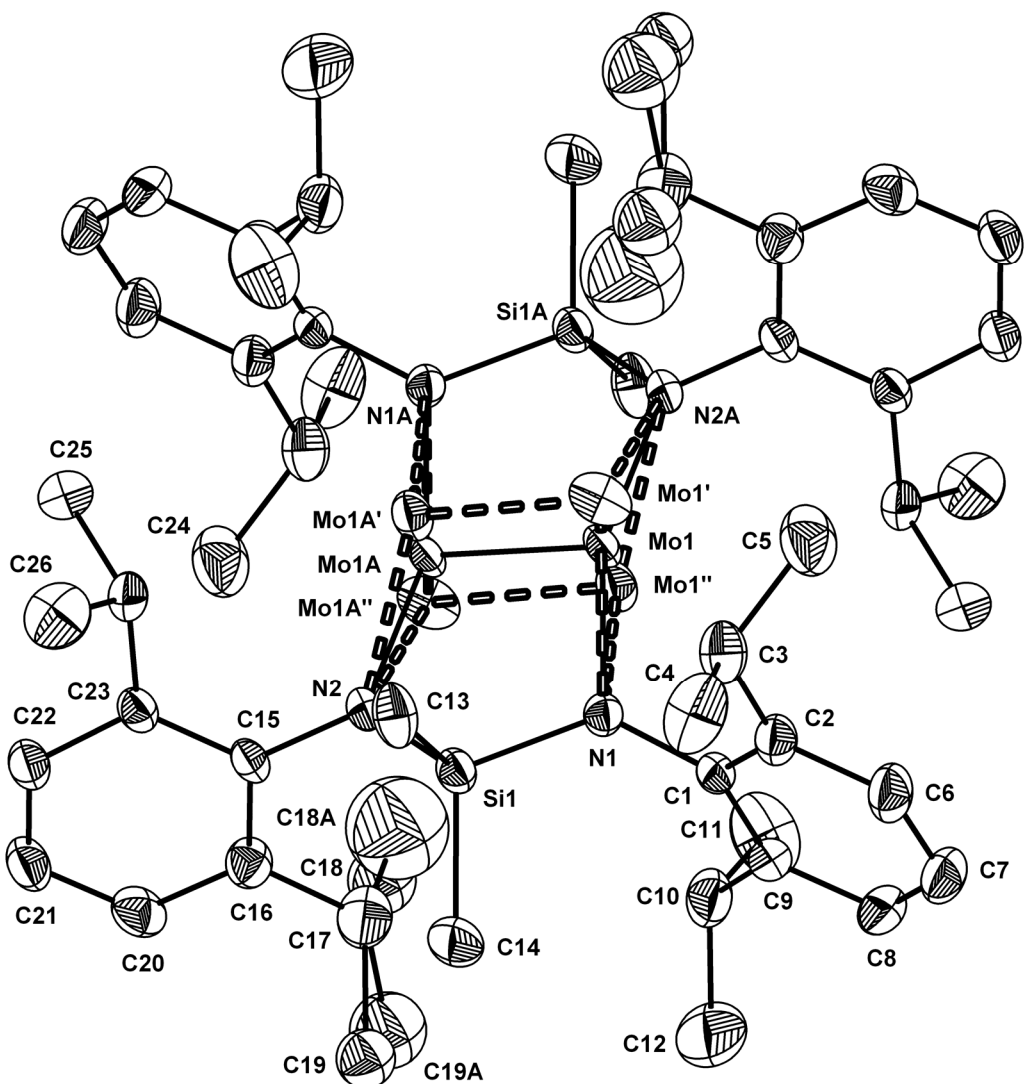


Figure S4. ORTEP diagram of complex 2 with ellipsoids at the 30% probability level and with the disorder of Mo₂ in three positions. The percentage occupancies for the three disordered Mo₂ units are 80%, 15%, and 5%.

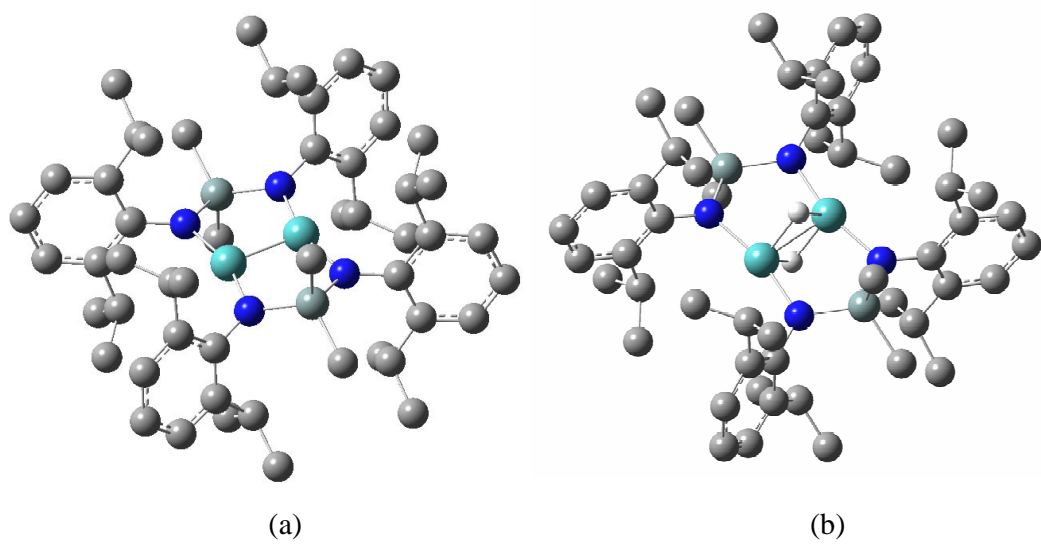


Figure S5. Computed **(a)** and **2(μ-H)₂** **(b)** with C_{2h} symmetry. The Mo–Mo distance of **(a)** and **(b)** is 2.168 and 2.381 Å, respectively.

Table S2. Comparison of several important geometrical parameters of **2** calculated by BLYP/LANL2DZ and BLYP/Basis I. This basis set I is constructed by triple- ζ 6-311G* over H, C, N and Si, plus LANL2DZ for Mo, resulting in 1406 Cartesian basis functions.

BLYP optimized geometrical parameters	Basis I	LANL2DZ
Cartesian basis functions	1406	728
symmetry	C_{2h}	C_{2h}
Mo–Mo bond length	2.168	2.168
Mo–N bond length ^b	2.049	2.039
N–Si bond length ^b	1.801	1.825
N–C bond length ^b	1.451	1.469
Si–C bond length ^b	1.901	1.908

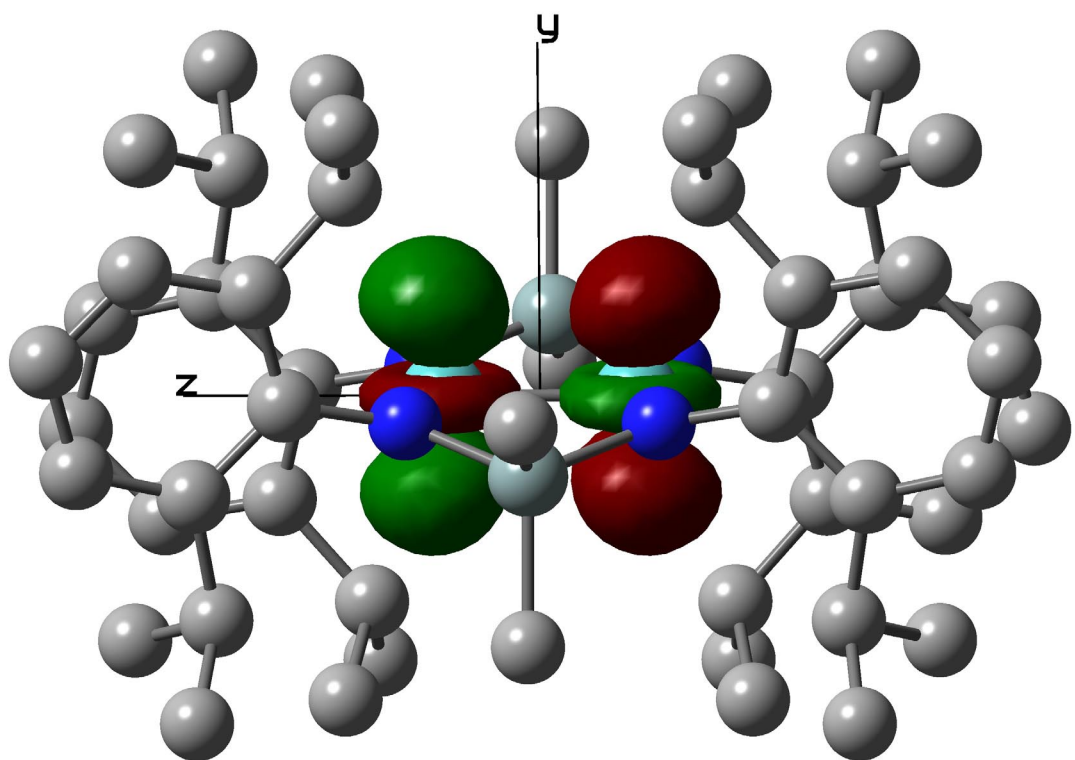


Figure S6. The contour plot of LUMO of **2**.

Table S3. Theoretical transitions with non-zero oscillator strengths of **2** using TD-BLYP/LANL2DZ/ ECP(LANL2).

Transition	Energy in eV	Energy in nm	Oscillator strength (<i>f</i>)
$^1\text{A}_g \rightarrow ^1\text{A}_u$	1.851	670	0.0639
$^1\text{A}_g \rightarrow ^1\text{B}_u$	2.155	583	0.0009
$^1\text{A}_g \rightarrow ^1\text{B}_u$	2.388	575	0.0157
$^1\text{A}_g \rightarrow ^1\text{B}_u$	2.453	519	0.0039

NBO analysis of 5 at BLYP/LANL2DZ/ECP(LANL2)

NATURAL POPULATIONS: Natural atomic orbital occupancies

NAO	Atom	No	lang	Type(AO)	Occupancy	Energy
1	Mo	1	S	Cor(4S)	1.97947	-2.21297
2	Mo	1	S	Val(5S)	0.50595	0.09539
3	Mo	1	S	Ryd(6S)	0.00135	13.04192
4	Mo	1	px	Cor(4p)	1.99431	-1.35126
5	Mo	1	px	Ryd(6p)	0.00200	0.72606
6	Mo	1	px	Ryd(5p)	0.00253	0.58705
7	Mo	1	py	Cor(4p)	1.99647	-1.38150
8	Mo	1	py	Ryd(6p)	0.00656	0.39334
9	Mo	1	py	Ryd(5p)	0.00155	0.34450
10	Mo	1	pz	Cor(4p)	1.98866	-1.37254
11	Mo	1	pz	Ryd(6p)	0.00151	2.72403
12	Mo	1	pz	Ryd(5p)	0.00192	2.04022
13	Mo	1	dxy	Val(4d)	0.74411	-0.11495
14	Mo	1	dxy	Ryd(5d)	0.00334	0.59602
15	Mo	1	dxz	Val(4d)	1.06067	-0.11130
16	Mo	1	dxz	Ryd(5d)	0.00717	0.65701
17	Mo	1	dyz	Val(4d)	1.04281	-0.13831
18	Mo	1	dyz	Ryd(5d)	0.00621	0.42967
19	Mo	1	dx2y2	Val(4d)	0.90249	-0.11055
20	Mo	1	dx2y2	Ryd(5d)	0.00511	0.68864
21	Mo	1	dz2	Val(4d)	1.04635	-0.15362
22	Mo	1	dz2	Ryd(5d)	0.00593	1.20267

(Occupancy) Bond orbital/ Coefficients/ Hybrids

1.	(1.99228) BD (1)Mo	1 -Mo 2				
	(50.00%)	0.7071*Mo	1 s(0.00%)p 0.00(0.01%)d 1.00(99.99%)			
			0.0000 0.0000 0.0000 0.0000 0.0026			
			-0.0018 0.0000 -0.0045 -0.0080 0.0000			
			0.0000 0.0000 0.0000 0.0000 0.3438			
			0.0165 0.9378 0.0450 0.0000 0.0000			
			0.0000 0.0000			
	(50.00%)	0.7071*Mo	2 s(0.00%)p 0.00(0.01%)d 1.00(99.99%)			
			0.0000 0.0000 0.0000 0.0000 0.0026			
			-0.0018 0.0000 -0.0045 -0.0080 0.0000			
			0.0000 0.0000 0.0000 0.0000 -0.3438			
			-0.0165 -0.9378 -0.0450 0.0000 0.0000			
			0.0000 0.0000			
2.	(1.99050) BD (2)Mo	1 -Mo 2				
	(50.00%)	0.7071*Mo	1 s(0.86%)p 0.03(0.02%)d 99.99(99.12%)			
			0.0007 -0.0917 -0.0136 0.0000 0.0000			
			0.0000 0.0000 0.0000 0.0000 -0.0003			
			0.0031 0.0149 -0.2217 -0.0158 0.0000			
			0.0000 0.0000 0.0000 0.3911 0.0193			
			0.8874 0.0310			
	(50.00%)	0.7071*Mo	2 s(0.86%)p 0.03(0.02%)d 99.99(99.12%)			
			0.0007 -0.0917 -0.0136 0.0000 0.0000			
			0.0000 0.0000 0.0000 0.0000 0.0003			
			-0.0031 -0.0149 -0.2217 -0.0158 0.0000			
			0.0000 0.0000 0.0000 0.3911 0.0193			
			0.8874 0.0310			
3.	(1.94449) BD (3)Mo	1 -Mo 2				
	(50.00%)	0.7071*Mo	1 s(0.00%)p 1.00(0.03%)d 99.99(99.97%)			
			0.0000 0.0000 0.0000 0.0002 0.0072			
			0.0030 -0.0002 0.0167 0.0029 0.0000			
			0.0000 0.0000 0.0000 0.0000 0.9380			
			-0.0322 -0.3441 0.0177 0.0000 0.0000			
			0.0000 0.0000			
	(50.00%)	0.7071*Mo	2 s(0.00%)p 1.00(0.03%)d 99.99(99.97%)			
			0.0000 0.0000 0.0000 0.0002 0.0072			
			0.0030 -0.0002 0.0167 0.0029 0.0000			
			0.0000 0.0000 0.0000 0.0000 -0.9380			
			0.0322 0.3441 -0.0177 0.0000 0.0000			
			0.0000 0.0000			
4.	(1.90658) BD (4)Mo	1 -Mo 2				
	(50.00%)	0.7071*Mo	1 s(30.30%)p 0.00(0.09%)d 2.30(69.61%)			
			0.0007 -0.5504 -0.0059 0.0000 0.0000			
			0.0000 0.0000 0.0000 0.0000 0.0001			
			0.0256 0.0159 -0.3678 0.0322 0.0000			
			0.0000 0.0000 0.0000 0.6156 -0.0445			
			-0.4205 0.0449			
	(50.00%)	0.7071*Mo	2 s(30.30%)p 0.00(0.09%)d 2.30(69.61%)			
			0.0007 -0.5504 -0.0059 0.0000 0.0000			
			0.0000 0.0000 0.0000 0.0000 -0.0001			
			-0.0256 -0.0159 -0.3678 0.0322 0.0000			
			0.0000 0.0000 0.0000 0.6156 -0.0445			
			-0.4205 0.0449			

Natural Bond Orbitals (Summary) :

NBO	Occupancy	Principal Delocalizations	
		Energy	(geminal, vicinal, remote)
<hr/>			
Molecular unit 1 (Mo2)			
1. BD (-1)Mo 1 -Mo 2	1.99228	-0.21757	425(r), 429(r), 433(r), 437(r) 581(r), 583(r), 351(r), 355(r) 359(r), 363(r), 353(r), 357(r) 361(r), 365(r), 367(r), 368(r) 369(r), 370(r), 463(r), 467(r) 471(r), 475(r)
2. BD (-2)Mo 1 -Mo 2	1.99050	-0.21845	218(g), 220(g), 233(r), 235(r) 424(r), 428(r), 432(r), 436(r) 658(r), 660(r), 662(r), 664(r) 545(r), 546(r), 547(r), 548(r) 423(r), 427(r), 431(r), 435(r) 367(r), 368(r), 369(r), 370(r) 385(r), 389(r), 393(r), 397(r) 505(r), 509(r), 513(r), 517(r)
3. BD (-3)Mo 1 -Mo 2	1.94449	-0.20292	277(r), 281(r), 263(r), 267(r) 271(r), 275(r), 280(r), 284(r) 577(r), 578(r), 579(r), 580(r) 233(r), 235(r), 423(r), 427(r) 431(r), 435(r), 278(r), 282(r) 581(r), 583(r), 261(r), 265(r) 269(r), 273(r), 262(r), 266(r) 270(r), 274(r), 367(r), 368(r) 369(r), 370(r), 463(r), 467(r) 471(r), 475(r), 415(r), 419(r) 385(r), 389(r), 393(r), 397(r) 658(r), 660(r), 662(r), 664(r) 351(r), 355(r), 359(r), 363(r) 352(r), 356(r), 360(r), 364(r) 461(r), 465(r), 469(r), 473(r)
4. BD (-4)Mo 1 -Mo 2	1.90658	-0.22059	248(g), 260(g), 239(g), 251(g) 261(r), 265(r), 269(r), 273(r) 233(r), 235(r), 243(g), 255(g) 262(r), 266(r), 270(r), 274(r) 277(r), 281(r), 582(r), 584(r) 424(r), 428(r), 432(r), 436(r) 247(g), 259(g), 264(r), 268(r) 272(r), 276(r), 417(r), 421(r) 280(r), 284(r), 577(r), 578(r) 579(r), 580(r), 713(r), 714(r) 715(r), 716(r), 609(r), 610(r) 658(r), 660(r), 662(r), 664(r) 278(r), 282(r), 463(r), 467(r) 471(r), 475(r), 385(r), 389(r) 393(r), 397(r), 423(r), 427(r) 431(r), 435(r), 353(r), 357(r) 361(r), 365(r), 383(r), 387(r) 391(r), 395(r), 386(r), 390(r) 394(r), 398(r), 462(r), 466(r) 470(r), 474(r), 623(r), 625(r) 627(r), 629(r), 425(r), 429(r) 433(r), 437(r), 597(r), 598(r) 599(r), 600(r), 655(r), 656(r) 375(r), 376(r), 377(r), 378(r) 325(r), 329(r)
<hr/>			
Total Lewis	79.75204	(96.5370%)	
Valence non-Lewis	2.79529	(3.3836%)	
Rydberg non-Lewis	0.06563	(0.0794%)	
<hr/>			
Total unit 1	82.61296	(100.0000%)	
Charge unit 1	1.38704		